

# Observation of Persistent Currents in Mesoscopic Connected Rings

W. Rabaud<sup>1</sup>, L. Saminadayar<sup>1</sup>, D. Mailly<sup>2</sup>, K. Hasselbach<sup>1</sup>, A. Benoît<sup>1</sup> and B. Etienne<sup>2</sup>

<sup>1</sup>Centre de Recherches sur les Très Basses Températures, B.P. 166 X, 38042 Grenoble Cedex 9, France

<sup>2</sup>Laboratoire de Microstructures et Microélectronique, B.P. 107, 92225 Bagneux Cedex, France

(February 5, 2020)

We report measurements of the low temperature magnetic response of a line of 16 GaAs/GaAlAs mesoscopic *connected* rings whose total length is much larger than  $l_\phi$ . Using an on-chip micro-SQUID technology, we have measured a periodic response, with period  $h/e$ , corresponding to persistent currents in the rings of typical amplitude  $0.40 \pm 0.08 nA$  per ring. Direct comparison with measurements on the same but *isolated* rings is presented.

PACS numbers: 73.23.-b, 73.20.Dx, 72.20.My

In a mesoscopic metallic sample, quantum coherence of the electronic wave functions can affect drastically the equilibrium properties of the system. In the case of a metallic ring in a magnetic field, the new boundary conditions imposed by the magnetic flux [1] lead the wave functions and therefore all the thermodynamic properties of the system to be periodic with flux, with periodicity  $\Phi_0 = h/e$  the flux quantum. One of the most striking consequence of this, first pointed out by Büttiker, Imry and Landauer [2] for the 1D case, is that a mesoscopic normal-metal ring pierced by a magnetic flux carries a persistent -non dissipative- current: this is a consequence of the periodicity of the free energy  $\mathcal{F}(\Phi)$  with flux, implying the existence of an equilibrium current  $I(\Phi) = -\partial\mathcal{F}(\Phi)/\partial\Phi$ . Subsequently, much theoretical effort has been devoted to the description of a realistic 3D disordered ring [3-7]. Both the sign and the amplitude of this current depend on the number of electrons in the ring and on the microscopic disorder configuration: thus this current, as other mesoscopic phenomena such as Aharonov-Bohm conductance oscillations [8], is sample specific. However, the order of magnitude of the current for a single, isolated ring can be characterized by its typical value  $I_{typ} = \sqrt{\langle I^2 \rangle}$ ,  $\langle \rangle$  denoting the average over disorder configurations. It is given [6,7] by  $I_{typ} = 1.56 I_0 l_e/L$ . In this formula,  $I_0 = ev_F/L$  where  $v_F$  is the Fermi velocity and  $L$  the perimeter of the ring, and  $l_e$  is the elastic mean free path: the current varies like the inverse of the diffusion time  $\tau_D = L^2/D$  where  $D = v_F l_e$  is the diffusion constant. When measuring an ensemble of rings, the typical current per ring decreases as  $1/\sqrt{N_R}$ , where  $N_R$  is the number of rings. At finite temperature [6,7,9], mixing of the energy levels reduces the current on the scale of the Thouless energy  $E_c$ , the energy scale for energy correlations. Further reduction arises when temperature reduces the phase coher-

ence length  $l_\phi$  down to values lower than  $L$ .

For a long time, persistent currents have been believed to be a specific property of isolated systems [2]. However, recent theoretical predictions suggest that persistent currents should exist even in connected rings: using a semi-classical model in the diffusive limit, ref. [10] calculated persistent currents in various networks of connected rings, showing that the amplitude of the persistent currents should be only weakly reduced as compared to its value in the same network of isolated rings. The reduction factor  $r = I_{connected}/I_{isolated}$  depends on the geometry of the network. For a line of connected rings separated by arms longer than  $l_\phi$ , a simple fraction  $r = 2/3$  has been predicted [10]; for the geometry considered here, it is expected [11] that  $r \approx 0.58$ . Moreover, this result is independent of the total size of the system, even much larger than  $l_\phi$ : this suggests that persistent currents could be observed in a macroscopic system. However, no experimental evidence of persistent currents in such a connected geometry has been reported up to now.

A couple of key experiments have confirmed the existence of persistent currents in isolated systems, either an ensemble of isolated rings [12-14], or a single isolated ring [15,16]. However, the amplitude of the currents found in ref. [12] and ref. [15], much larger than expected, is still not understood: in this context, the need for new experiments to clarify these results and provide new experimental facts is very important. Moreover, the existence of persistent currents in a network of connected rings larger than  $l_\phi$  remains to be experimentally demonstrated.

In this Letter, we report on measurement of the low temperature magnetic response of a line of 16 GaAs/GaAlAs *connected* rings. The sample is designed so that its total size is much larger than  $l_\phi$ , while the perimeter of each ring is smaller than  $l_\phi$ . We have developed a new experimental setup based on a multi-loop  $\mu$ -SQUID gradiometer, and observed a periodic response of the magnetization with period  $\Phi_0 = h/e$ , corresponding to persistent currents in the rings of amplitude  $0.40 \pm 0.08 nA$  per ring, in good agreement with theory. Using gates, we performed measurement on the same but *isolated* rings: we have also observed an  $h/e$  periodic signal, corresponding to persistent currents in the rings whose amplitude is similar to the one observed for connected rings.

The GaAs/GaAlAs heterojunction was grown using molecular beam epitaxy. The structure of the epilayers is  $1 \mu m$  GaAs buffer layer,  $15 nm$  GaAlAs spacer layer,

48 nm Si doped GaAlAs layer and 5 nm GaAs cap layer. At 4.2 K in the dark, the two dimensional electron gas (2DEG) at the heterointerface has an electron density of  $5.2 \times 10^{11} \text{ cm}^{-2}$  and a mobility of  $0.8 \times 10^6 \text{ cm}^2 \text{ V}^{-1} \text{ s}^{-1}$ . This yields a Fermi velocity  $v_F = 3.16 \times 10^5 \text{ m s}^{-1}$  and a Fermi wavelength  $\lambda_F = 35 \text{ nm}$ . All the lithographic operations are performed using electron beam lithography on PMMA (polymethyl methacrylate) resist with a JEOL 5DIIU electron beam writer. We first pattern an aluminium mask of the rings before etching 5 nm of the GaAs cap layer by ion milling with 250 V argon ions. This is sufficient to deplete the underlying 2DEG. The rings, actually squares of internal side length  $2 \mu\text{m}$ , external side length  $4 \mu\text{m}$ , mean perimeter  $L = 12 \mu\text{m}$ , connected by  $2 \mu\text{m}$  long arms, are connected to AuGeNi ohmic contacts in a two-probe geometry. Using a similar technique we have fabricated wires of different widths to characterize the sample after etching. For wires of similar width, we have measured a phase coherence length  $l_\phi \approx 20 \mu\text{m}$  derived from weak localisation. Conductance measurements give an elastic mean free path of  $l_e \approx 8 \mu\text{m}$ , and a depletion length of 100 nm on each side of the wire due to the etching process. Therefore the effective width of the arms of our rings is  $W = 0.8 \mu\text{m}$ . It should be noted that in this experiment, we are not in the pure diffusive case since  $l_e \lesssim L$ , but it is expected that the analytical results for the diffusive case still apply [17].

Three Schottky gates are then deposited allowing to deplete the 2DEG underneath. The first one (labeled " $G_1$ " in fig.1) is deposited on the top of each ring and allows to suppress all the interference effects in the rings such as the persistent currents. The second gate (labeled " $G_2$ " in fig.1) is deposited on the two outgoing wires (labeled " $\Omega$ " in fig.1) and make possible the insulation of the rings from the ohmic contacts. The last one (labeled " $G_3$ " in fig.1) is placed on the arms joining two rings, allowing the measurement of isolated rings. A calibration loop (labeled "*calib. loop*" in fig.1) with the same dimensions as a ring is patterned in order to calibrate our experimental setup. Gates and calibration loop are obtained by liftoff of 10 nm titanium and 50 nm gold films. The device is then covered with a 60 nm insulating layer (AZ 1350 resist baked at  $170^\circ\text{C}$ ).

The next step is the fabrication of the  $\mu$ -SQUID. It is designed as a gradiometer, equivalent to a two counter-wound loops, in order to compensate the external magnetic flux [16,18]. The first level (see fig.1) is deposited on the top of the rings and of the calibration loop. Then a new insulating layer is deposited and the gradiometer is closed with the other half. The two Dayem micro-bridge Josephson junctions,  $300 \text{ nm} \times 50 \text{ nm} \times 30 \text{ nm}$ , are lithographically defined at this stage. The contact between the two aluminium levels is obtained by covering them with aluminium pads deposited after an ion bombardment cleaning. The first  $\mu$ -SQUID layer is made of

60 nm thick aluminium and the second one, containing the two Dayem micro-bridges, of 30 nm thick aluminium in order to reduce the critical current of the  $\mu$ -SQUID. As the  $\mu$ -SQUID has exactly the same shape as the rings, the coupling between them is almost perfect [18].

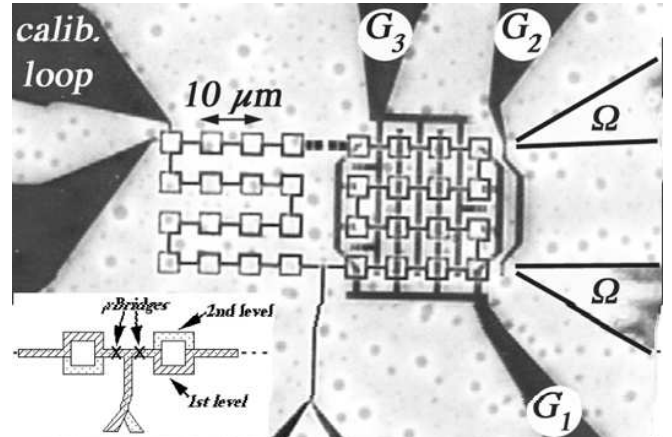


FIG. 1. Optical photograph of the sample.  $G_1$ ,  $G_2$  and  $G_3$  are the three Schottky gates. The calibration loop (on the left side) calibrates the  $\mu$ -SQUID response. The visible squares are the  $\mu$ -SQUID and the GaAs/GaAlAs rings are under the right side of the  $\mu$ -SQUID. The mean perimeter of one ring is  $12 \mu\text{m}$ , and the length of the arms between two rings is  $2 \mu\text{m}$ . The total "length" of the 16 connected rings (perimeters + arms) is  $0.22 \text{ mm}$ . Inset shows how the  $\mu$ -SQUID is designed to form a gradiometer.

Design considerations and the accuracy of the e-beam lithography allow a compensation of the external magnetic flux of 99.96%. In order to avoid flux penetration in the Al layers of the  $\mu$ -SQUID, we limit the sweep of the magnetic field to 35 G, corresponding to  $3 \Phi_0$  and  $9 \Phi_0$  in each ring for the inside and outside trajectories respectively. The critical current of the  $\mu$ -SQUID is measured using dedicated electronics which ramps a dc current until the  $\mu$ -SQUID's critical current is attained [18]. The current is then reset, and the value of the critical current sent to a computer. This cycle is repeated periodically at 5 kHz, and the measured flux resolution of our gradiometer is then  $\approx 5 \times 10^{-4} \Phi_0 / \sqrt{\text{Hz}}$ .

Resistance measurements are performed separately using a conventional ac lock-in technique, with an ac current of 100 pA at 777 Hz. The resistance of the sample ( $\approx 10 \text{ k}\Omega$  at 0 field) is measured as a function of the magnetic field which is swept from  $-33.5 \text{ G}$  to  $-3.5 \text{ G}$ . In this range of magnetic field, the external magnetic flux is almost perfectly compensated. Fig.2 shows the square root of the power spectrum of the resistance measured at 20 mK, obtained by Fast Fourier Transform (FFT) of the data. The horizontal scale shows the field frequency expressed in  $\text{G}^{-1}$ . Because of the aspect ratio of the rings, the  $\Phi_0$  frequency extends from  $0.12 \text{ G}^{-1}$  to  $0.35 \text{ G}^{-1}$ . The spectrum clearly exhibits a peak in the  $\Phi_0$  frequency range, corresponding to Aharonov-Bohm con-

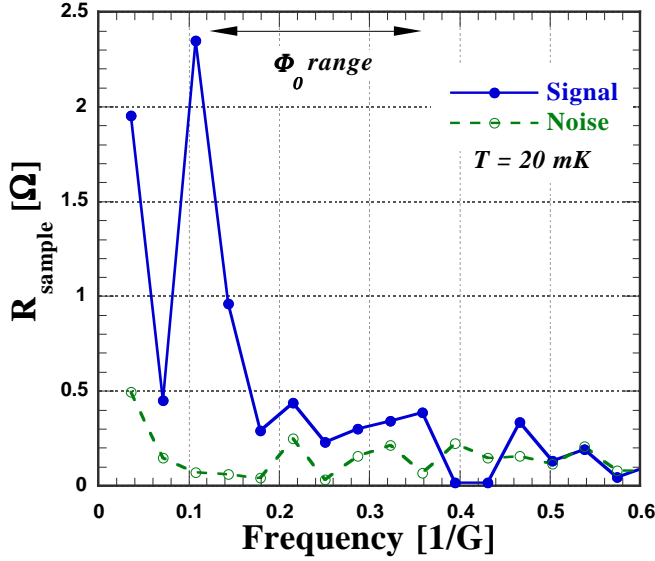


FIG. 2. Typical power spectrum of the Aharonov-Bohm conductance oscillations in a line of 16 rings, measured at 20 mK. Arrows indicate the  $\Phi_0$  frequency window, calculated from the geometrical parameters of our sample. The Aharonov-Bohm peak is just one point out of this window, due to the discretization on the frequency axis. Open circles correspond to experimental noise, i.e. FFT of the difference between measurements with rings closed. Solid circles correspond to experimental signal, i.e. FFT of the measurement with the rings closed. Increase of the signal at low frequency is due to weak localisation and universal conductance fluctuations, which are cancelled in the "noise" measurements.

ductance oscillations. The separation between each point of the FFT is directly related to the range of magnetic field used, which leads to a discretization of  $0.036 G^{-1}$  on the frequency axis.

To measure the persistent currents, the critical current of the  $\mu$ -SQUID is measured as a function of the magnetic field, again swept from  $-33.5 G$  to  $-3.5 G$  at  $7.5 G s^{-1}$ . The sensitivity to the currents in the rings is calibrated using the calibration loop. We perform measurements with the rings "opened" and "closed" ( $-561 mV$  applied on the gate  $G_1$  when measuring opened rings). The rings are insulating from the ohmic contacts by applying  $-558 mV$  on the gate  $G_2$ . The periodic sequence of measurements is  $O_1 O_2 C_1 C_2 O_3 O_4 C_3 C_4 \dots$ , where  $O_x$  denotes a measurement with the rings opened, and  $C_x$  a measurement with the rings closed. Each measurement represents about 1 min of accumulation time. The signal of persistent currents is then extracted by Fast Fourier Transform (FFT) of the difference between measurements with closed and opened rings,  $((C_1 - O_2) + (C_2 - O_3))$ , whereas the noise is obtained by FFT of the difference between two identical measurements,  $((C_1 - C_2) + (O_1 - O_2))$ . Such a possibility of background noise subtraction is an important advantage of our experimental technique. The total signal is divided by 16 to obtain the current per ring.

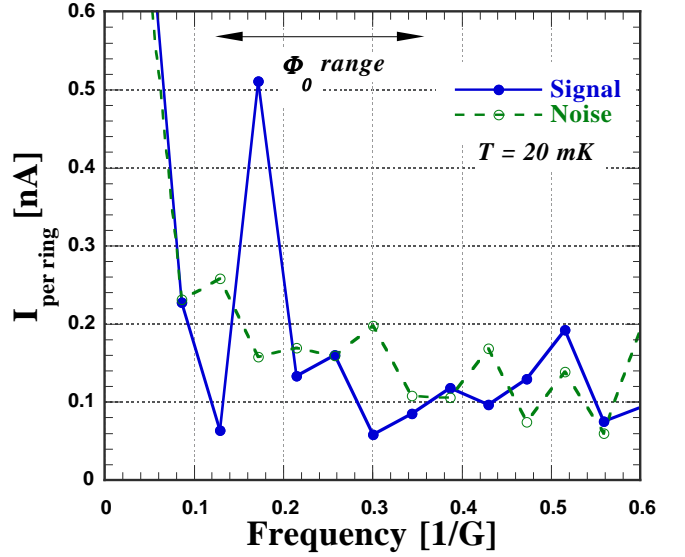


FIG. 3. Typical power spectrum of the magnetization due to persistent currents in a line of 16 connected rings expressed in nA per ring, measured at 20 mK. Arrows indicate the  $\Phi_0$  frequency window, calculated from the geometrical parameters of our sample. Open circles correspond to experimental noise, i.e. differences between two identical measurements. Solid circles correspond to experimental signal, i.e. differences between measurements with the rings closed and opened.

Typical result for the square root of the power spectrum of the persistent currents expressed in nA per ring is depicted in fig.3. The increase of the signal at low frequency is mostly due to slow temporal fluctuations of the critical current of the  $\mu$ -SQUID. Note that contrary to previous experiments [16], the aspect ratio of the rings allows the signal to extend over several units of the FFT abscissa, corresponding to the  $\Phi_0$  frequency range [8]: the amplitude of the persistent currents is then obtained by taking the difference between the area under the  $\Phi_0$  region of the "signal" and the "noise" curves. By this means the amplitude of the "signal" curve in the  $\Phi_0$  frequency range of fig.3 is a clear signature of persistent currents in our line of connected rings.

It should be stressed that random modifications of the disorder configuration of the sample occurs due to relaxation processes of the dopants in the GaAlAs layer; this explains why the observed signal varies in time. However, this instability allows to perform statistics over the amplitudes of the persistent currents found in different measurements, equivalent to different disorder configurations, and thus to measure the typical current [16]. Using this technique, we find for our line of 16 connected rings a typical current of  $0.40 \pm 0.08 nA$  per ring. This value is in good agreement with the theoretical value  $0.58 \times 1.56 (I_0/\sqrt{N_R}) (l_e/L) \approx 0.63 nA$  per ring,  $r = 0.58$  being the reduction factor predicted for the same line of connected rings and  $I_0$  being derived from our experimen-

tal parameters. Note that strictly speaking the model used in ref. [10] is valid only in the diffusive regime; in our samples  $l_e \lesssim L$ , and deviations from the pure diffusive case may be expected [11]. Finite value of  $l_\phi$  [7] as well as the exact shape of the sample (squares instead of rings) may also account for the difference between theoretical and experimental values. Finally, contrary to recent experiment on gold rings [14], the  $h/2e$  component due to time reversal paths is not observed either in the Aharonov-Bohm conductance oscillations or in the persistent currents, within the experimental uncertainty: this may be due to the fact that such time reversal paths are less numerous in quasi-ballistic samples than in diffusive ones.

By applying  $-540\text{ mV}$  on the gate  $G_3$ , which is sufficient to deplete the arms between the rings, we isolated the rings and performed the same experiment as for connected rings. We also observed an  $h/e$  periodic signal, corresponding to persistent currents in the rings of  $0.35 \pm 0.07\text{ nA}$  per ring, to be compared with the theoretical value  $1.56 (I_0/\sqrt{N_R}) (l_e/L) \approx 1.09\text{ nA}$  per ring. As mentioned above, finite value of  $l_\phi$  may account for the difference between experimental and theoretical values.

The key point is the direct experimental comparison between persistent currents in the same rings either connected or isolated. Our experiment gives a ratio  $I_{\text{connected}}/I_{\text{isolated}}$  between 0.76 and 1.81. The theoretical value calculated by ref. [10,11] is  $r \approx 0.58$ ; if not equal, both values are of order unity. This points out the most striking result of our experiment: *persistent currents are not significantly modified when connecting or isolating the rings*. All previous experiments have been carried out on isolated rings [12–16]. Our result shows that persistent currents are not a specific property of isolated systems: in our line of rings, electrons can visit the whole sample and lose their phase coherence. However, we showed quantitatively that the trajectories encircling individual loops, even when loops are connected, form the main contribution to the persistent currents. By extension, this suggests that persistent currents could be observed in a macroscopic sample: all the closed trajectories smaller than  $l_\phi$ , which enclose flux, should give rise to a measurable persistent current, even if the whole sample is clearly not a quantum coherent object.

In conclusion, using a multiloop  $\mu$ -SQUID gradiometer, we have measured the magnetization of a line of connected GaAs/GaAlAs rings as a function of magnetic field. We have observed a periodic response, with period  $h/e$  in the rings; amplitude of the corresponding persistent currents is in good agreement with theoretical estimates. Measurements on the same but isolated rings also showed oscillatory component of the magnetization with period  $h/e$ : *amplitude of persistent currents in connected and isolated rings has been found to be similar*.

Further measurements on various geometries are now needed to fully understand the effect of the connectivity

of the sample on the persistent currents. Experiments in the pure diffusive case or on a larger number of rings should also help to give a correct description of this "extensive" nature of persistent currents. From the theoretical side, a model for the ballistic case is needed for a direct comparison with our experiment.

Fruitful discussions with G. Montambaux, M. Pascaud, H. Bouchiat and P. Butaud are acknowledged. We thank J. L. Bret, G. Simiand, J. F. Pini and H. Rodenas for technical help, and D. K. Maude for careful reading of the manuscript.

- 
- [1] N. Byers and C. N. Yang, Phys. Rev. Lett. **7**, 46 (1961).
  - [2] M. Büttiker, Y. Imry and R. Landauer, Phys. Lett. **96A**, 365 (1983).
  - [3] H. Bouchiat and G. Montambaux, J. Phys. France **50**, 2695 (1989); G. Montambaux, J. Phys. I France **6**, 1 (1996).
  - [4] V. Ambegaokar and U. Eckern, Phys. Rev. Lett. **65**, 381 (1990).
  - [5] B. Altshuler, Y. Gefen and Y. Imry, Phys. Rev. Lett. **66**, 88 (1991); F. von Oppen and E. K. Riedel, Phys. Rev. Lett. **66**, 84 (1991); A. Schmid, Phys. Rev. Lett. **66**, 80 (1991).
  - [6] H. F. Cheung, E. K. Riedel and Y. Gefen, Phys. Rev. Lett. **62**, 587 (1989); N. Argaman, Y. Imry and U. Smilansky, Phys. Rev. B **47**, 4440 (1993); E. K. Riedel and F. von Oppen, Phys. Rev. B **47**, 15449 (1993).
  - [7] G. Montambaux, in *Quantum Fluctuations*, S. Reynaud, E. Giacobino and J. Zinn-Justin eds., Amsterdam (1997) and references therein.
  - [8] S. A. Washburn and R. A. Webb, Adv. Phys. **35**, 375 (1986).
  - [9] R. Landauer and M. Büttiker, Phys. Rev. Lett. **54**, 2049 (1985).
  - [10] M. Pascaud and G. Montambaux, Europhys. Lett. **37**, 347 (1997); Phys. Rev. Lett. **82**, 4512 (1999).
  - [11] G. Montambaux, private communication.
  - [12] L. P. Lévy, G. Dolan, J. Dunsmuir and H. Bouchiat, Phys. Rev. Lett. **64**, 2074 (1990); L. P. Lévy, D. H. Reich, L. Pfeiffer and K. West, Physica B **189**, 204 (1993).
  - [13] B. Reulet, M. Ramin, H. Bouchiat and D. Mailly, Phys. Rev. Lett. **75**, 124 (1995); Y. Noat, H. Bouchiat, B. Reulet and D. Mailly, Phys. Rev. Lett. **80**, 4955 (1998).
  - [14] P. Mohanty, Ann. Phys. (Leipzig) **8**, 549 (1999).
  - [15] V. Chandrasekhar, R. A. Webb, M. J. Brady, M. B. Ketchen, W. J. Gallagher and A. Kleinsasser, Phys. Rev. Lett. **67**, 3578 (1991).
  - [16] D. Mailly, C. Chapelier and A. Benoit, Phys. Rev. Lett. **70**, 2020 (1993).
  - [17] G. Montambaux, H. Bouchiat, D. Sigeti and R. Friesner, Phys. Rev. B **42**, 7647 (1990).
  - [18] K. Hasselbach, C. Veauvy and D. Mailly, Physica C **332**, 140 (2000).